# IMAGE-BASED GROUND VELOCITY MEASUREMENT

M. L. Stone, G. A. Kranzler
MEMBER ASAE MEMBER ASAE

## ABSTRACT

A prototype ground speed measuring system was developed. The device uses successive images of the ground taken from a moving vehicle to determine vehicle speed. Operating characteristics of the system were determined. Accuracy of the device was found to be about 2% of the reading. Artificial lighting was needed to allow operation in dim or night conditions.

**KEYWORDS.** Ground speed, Image processing, Machine vision.

## INTRODUCTION

The need for more efficient agricultural machines has made accurate speed measurement a necessity. Modern planting, fertilizing, and chemical application equipment requires accurate speed measurement for effective area-based metering. Similarly, traction system efficiencies are critically linked to wheel slip and require absolute ground speed measurements for effective monitoring. Future agricultural machines may require distance measuring to allow field positioning and position-tailored farming.

Time-tested techniques are available for speed or distance measurement. The simplest speed transducers are wheel-driven encoders. Planters, for example, employ mechanical distance measuring to control seeding rate. Accuracy of wheel driven devices is subject to wheel slippage (Tompkins et al., 1988), variation of rolling radius, mud and dust interference, and wear. Tompkins et al. found errors in speed measurement of between 4 and 10% in non-driven, uncalibrated wheels.

Developments in modern electronics allow more accurate and flexible monitoring and control to be exercised on agricultural systems. Doppler radar (Sokol, 1984), which offers the advantage of non-contact speed measurement, has emerged as an alternative to wheel driven devices. Although gaining in acceptance, doppler radar devices are somewhat limited by high cost, loss of accuracy at low speeds, and sensitivity to moving vegetative ground cover. Field testing has demonstrated radar-based measurements to estimate average velocities to within 1% on crop-free surfaces (Tompkins et al., 1988). They also found variations as high as 8% when the radar was required to use tall crop cover as a ground reference.

Image-based speed measurement has the potential to overcome low-speed limitations of doppler radar and could be used with accuracy in tall crop cover. An image-based system uses successively acquired ground images to obtain displacement. The imaging system is mounted on a moving machine and focused on the ground. Consecutive overlapping images are acquired with a solid-state imaging system. Displacement of objects in consecutive images may be proportional to displacement of the machine. A computer is used to gather and analyze the successive images and to compute displacement and speed.

## PREVIOUS WORK

The technical and economic feasibility of imaging for velocity measurement is founded on the development of solid-state imaging devices and efficient algorithms for image processing. Flory (1985) reviews the rapid advances in solid-state image acquisition technology and predicts continued progress. Development and improvement of image processing algorithms related to displacement detection and speed measurement are reviewed by Mussman et al. (1985). They show the close similarity of displacement estimation algorithms, which typically use a displaced frame difference (DFD) technique. The DFD technique matches two image segments by minimizing the intensity difference between images, with respect to displacement between the images. The technique can be thought of in terms of least squares curve fitting. One image is superimposed on the other until the sum of the squares of the differences between intensities is minimized. Mussman et al. also show that minimizing the DFD corresponds to maximizing cross-correlation, the classical technique for matching time-based signals.

Barnea and Silverman (1972) introduce algorithms for similarity detection in images and apply them to displacement detection. They also point out the computational advantage of using a differencing technique over Fast Fourier Transform (FFT) methods and cross-correlation. Their algorithms utilize the rate of accumulation of error in calculation of the DFD to reduce computation time. In their technique, the summation is begun and the rate of error accumulation is tracked. Rapid accumulation of error indicates a poor fit and allows early rejection of a particular displacement. Reductions in computation time were conservatively estimated to be 50% over FFT correlation and greater than 50% for direct correlation.

Article has been reviewed and approved for publication by the Electrical and Electronic Systems Div. of ASAE. Presented as ASAE Paper No. 85-3040.

Reference to commercial products or trade names is with the understanding that no discrimination is intended and no endorsement is implied.

The authors are **Marvin L. Stone,** Associate Professor, and **Glenn A. Kranzler,** Professor, Dept. of Agricultural Engineering, Oklahoma State University, Stillwater.

  0001-2351 / 92 / 3505-1729 

### Objective

The objective of this study was to design, test, and characterize the performance of an imaging-based velocity measuring system.

## Design

The initial design concept for the velocity detection system was to use a solid-state imaging integrated circuit to acquire successive ground images from a moving machine. Data from the imaging chip would then be transmitted to a microprocessor-based computer for data processing and display of speed. The microprocessor-based system would provide internal time measurement.

Solid-state imaging devices are constructed to allow an image to be focused directly on a silicon substrate. The substrate has photo-sensitive sites arranged across the surface of the substrate. Each site produces a signal proportional to intensity of incident light. The image is represented by signals from individual picture elements, or pixels. A linear imaging device was selected for the design, with an arrangement of 256 pixels × 1 pixel wide. The resulting device could be secured to a moving machine on which the line image was aligned parallel with the direction of travel. As successive line images were acquired, the overlapping sections could be identified. figure 1 shows the geometry of the resulting system.

### Error Analysis

Error in measurement was an important factor in the design. An error analysis demonstrated the effects of time and displacement measurement on total error in speed. Using the techniques of Hall (1977), the square of total error in speed measurement was:

$$\varepsilon^2 = \left(\frac{\partial v}{\partial t}\right)^2 \varepsilon_t^2 + \left(\frac{\partial v}{\partial x}\right)^2 \varepsilon_x^2 \qquad (1)$$

where

$\varepsilon_X$ = displacement error
v = velocity
$\varepsilon_t$ = time error
$\varepsilon$ = error in velocity

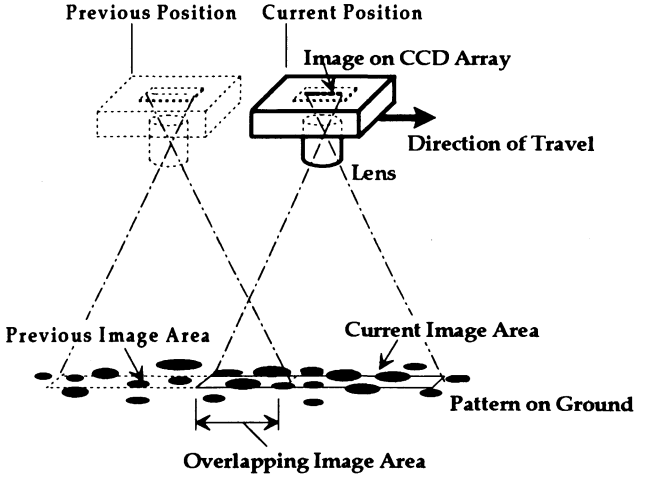


**Figure 1–Geometry of the image-based velocity measuring system.**

After performing the operations indicated in equation 1, and assuming velocity is displacement divided by time, the total error becomes:

$$\varepsilon^2 = \left(\frac{x^2}{t^4}\right) \varepsilon_t^2 + \left(\frac{1}{t^2}\right) \varepsilon_x^2 \qquad (2)$$

Error in time is very small using the crystal-controlled clock in a microprocessor system, and the time error term is negligible for reasonable geometry and velocities. Total error squared is then shown in equation 3.

$$\varepsilon^2 \cong \left(\frac{1}{t^2}\right) \varepsilon_x^2 \qquad (3)$$

Taking the square root of both sides of equation 3, error in speed is shown to be proportional to the error in the displacement measurement divided by time. Taking measurements over a longer time will decrease error, but error in displacement will be the primary determinant of total system error. For the linear array system, the number of pixels deviating from the expected displacement divided by the pixel displacement will determine the error in speed. Assuming an overlap or displacement of 128 pixels and an error in matching images of ±1 pixel, errors of less than 1% could be expected for velocity.

The initial concept was carried through to prototype. The design consisted of three hardware components and software. Hardware components were the imaging chip and support hardware, the data acquisition component, and the microcomputer component.

### Hardware

A design development board available from Fairchild Camera and Instrument Corporation was used to provide the imaging chip and support hardware. The board included a Fairchild CCD111, a charge coupled device (CCD) solid-state imaging chip and necessary clock support components. The 10 × 12 cm board was mounted in an aluminum frame and fitted with an f2.8, 35 mm focal length lens.

A hardware image acquisition system (frame grabber) was required to retrieve images from the Fairchild CCD. Analog video signals from the Fairchild chip were clocked out at a minimum frequency of 500 kHz. Initial testing revealed that the digitized image required quantitization in more than one bit (a binary image). With binary images and low contrast, an all-white or all-black image was likely and prevented image matching. In addition, the data rate from the chip exceeded the data transfer rate of simple microprocessor-based systems. Parallel input at rates of 1 MHz was required. A frame grabber was designed to accommodate the speeds. Figure 2 shows a block diagram of the frame grabber. A Telemos 7-bit flash converter was teamed with a 2 K × 8-bit CMOS RAM chip and clocking logic allowing as many as eight line images to be digitized and stored before processing. The frame grabber was interfaced to the microcomputer through 8-bit parallel ports. The microcomputer would initiate the acquisition of an image, accept a confirmation signal, and retrieve the image from the RAM chip.

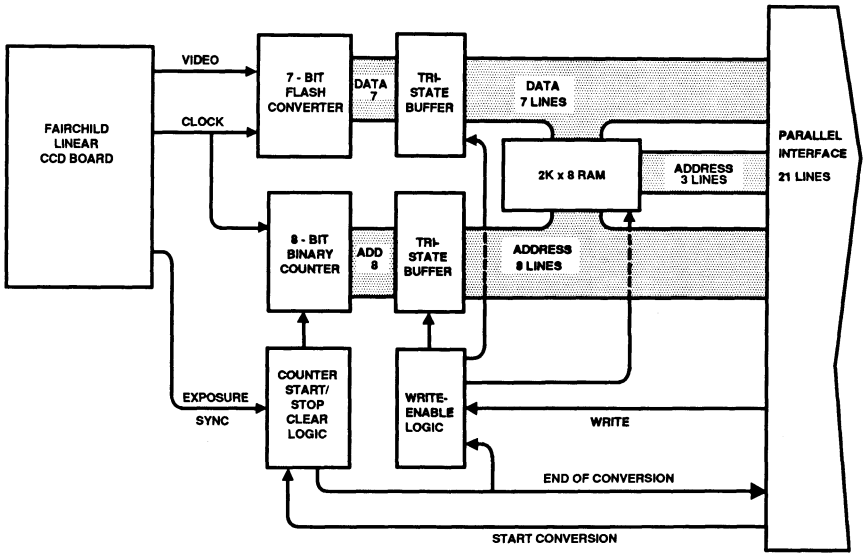


**Figure 2–Block diagram of frame grabber.**

A Motorola EXORbus single-board microcomputer was used to process the image data. The EXORbus board utilized an MC6809 microprocessor to execute the image processing algorithms contained in on-board firmware. A bus-based prototype board was used as a foundation for the data acquisition component of the system. The board contained the flash converter, RAM, parallel ports, and bus interface.

## Software

Software design was critical in obtaining satisfactory performance from the system. Routines were developed to acquire images, process the image data, and display the resulting velocity. In operation, the software signaled the frame grabber to acquire an image. After the image had been acquired, the software was used to transfer the digitized image into local RAM on the single-board computer. The digitized image consisted of 256 successive bytes, each containing 7 bits of significant data. The value in each byte corresponded roughly with the luminance of the image as detected by the CCD111 circuit.

Two algorithms were tested to process successively acquired images. The first was an adaptation of direct correlation described by Barnea and Silverman (1972). Their technique was implemented for 8-bit wide data and 16-bit accumulations. Summation of absolute value was used instead of squaring and was implemented by controlling subtraction order. The minimum of the DFD was found by computing the sum of the absolute value of luminance difference between frames. The sum was computed for each of the possible displacements, and a running record of the minimum was maintained. Equation 4 describes the process.

$$\min \mathrm{DFD}(k) = \sum_{i=1}^{i=128} \min\left(\left|A(i) - B(i+k)\right|\right) \quad (4)$$

where

i = pixel position

k = displacement of the "B" image with respect to "A"

A = luminance of the initial image

B = luminance of the second image

An alternative algorithm was developed as an elaboration of the first. This variation was a form of early rejection of large-error DFD, as suggested by Barnea and Silverman (1972). Summation at a particular displacement (k) was halted when the sum was greater than a specified threshold value. The threshold was set above the expected minimum, and calculations were avoided when they would not determine a minimum. A further improvement was made in the algorithm by moving the threshold to any complete summation less than the present threshold during summations for a particular image.

All of the time-critical software was coded in 6809 assembly language. A menu-based supervisory program was coded in C. The algorithms were also coded in 68000 assembly language to evaluate execution time reductions using a faster processor.

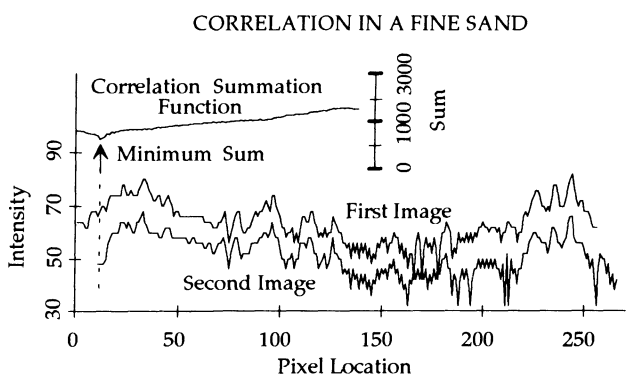


**Figure 3–Typical correlation curves. Second image is shifted to the right as suggested by the correlation summation minimum, and shifted down by 20 units to allow images to be compared.**

## TESTING

The prototype was tested to determine accuracy, illumination requirements, and potential velocity sampling rate. Three areas were investigated in evaluating accuracy of the prototype; accuracy without misalignment, accuracy with angular misalignment, and accuracy with side-slip misalignment. Angular misalignment would be expected to occur in practical systems when vehicles turn corners. The second image snapped would be rotated and translated with respect to the first image. A similar problem was envisioned due to side-slip of the vehicle. Movement of the vehicle perpendicular to the normal line of travel would prevent the second image in a pair from overlapping with the first. Both types of misalignments were expected to result in images that could not be matched and prevented the system from detecting speed.

## ACCURACY

Accuracy without misalignment was evaluated by fixing the imaging system 0.64 m (25 in.) above a textured surface. The textured surface, either a cloddy red soil or a fine sand, was mounted on a linear precision table which enabled accurate and repeatable displacements. Care was taken to focus the image using an oscilloscope to observe the image signal. Optical alignment was accomplished by using a striped target and observing the alignment pattern on the oscilloscope. Typical signals from a successive pair of images and the correlation curve are plotted in figure 3. The effective image length on the soil or sand was 0.05 m (2 in.). Error was found to be consistently ±2 pixels displacement.

Accuracy without misalignment was also tested on a moving target. A red cloddy soil was glued to a rubber belt. An apparatus was constructed to drive the belt at precise speeds. A tab attached to the belt was used to interrupt the beam on a light-emitting diode/light-detector diode pair. A digital timer/frequency counter was used to measure the average belt speed. Velocities in the 0.31 to 3.10-m/s (1 to 10-mph) range were tested. Error with the moving target was also found to be ±2 pixels displacement.

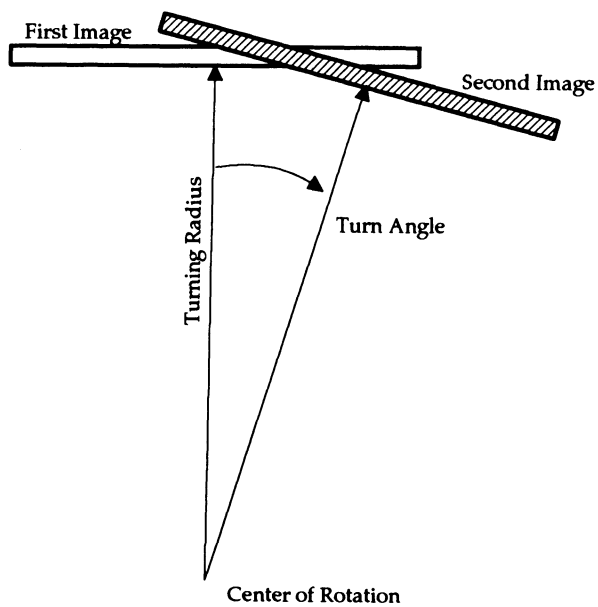


**Figure 4–Geometry for angular misalignment measurement.**

**TABLE 1. Effect of side-slip on error**

| Displacement (m) | Side-Slip (m) | Measured Pixel Dispacement* Left Slip | Right Slip |
|---|---|---|---|
| 0.013 | 0.0 | 55 | 55 |
| 0.013 | 0.000 3 | 56 | 55 |
| 0.013 | 0.000 5 | 56 | 55 |
| 0.013 | 0.000 8 | 56 | 55 |
| 0.013 | 0.001 0 | 55 | 112 |
| 0.013 | 0.001 3 | 55 | 113 |
| 0.013 | 0.001 5 | 17 | 112 |

* Expected displacement was 55 pixels.

Accuracy with angular misalignment was evaluated as in the first test, but a rotary precision table was substituted. The soil surface was mounted on an arm extending from the table. The point of displacement measurement was selected at various radii from the rotation center as shown in figure 4. Error was found to be either within the ±2 pixel range, or no image match could be found. Error was observed to be only a function of the angle of rotation. No difference was found with different soil types. Angles greater than 0.9 degrees produced no match, while angles of 0.9 degrees or less resulted in a ±2 pixel error. The 0.9-degree limit allowed up to 0.03-m (1-in.) displacements to be measured at turning radii as small as 2.0 m (78 in.).

Accuracy with side-slip misalignment was also evaluated. Tests were conducted with an X-Y linear table. The table was adjusted for displacement. Side-slip was then applied at an angle perpendicular to the displacement. misalignment was applied in both side-slip directions.

As above, tests were run with cloddy red soil and with sand. No differences in performance were found between soil types. Table 1 shows results of a typical test. The difference between left and right slip was attributed to offset initial centering.

All tests showed large errors when side-slip exceeded 0.000 77 m (0.03 in.) or 1.5% of the image length. The allowable side-slip for the system was approximately 6% of the displacement.

## ILLUMINATION REQUIREMENTS

Illumination requirements of the system were measured with a Mamiya-Sekor 35 mm SLR camera light meter calibrated with a Gossen Panlux luxmeter. The camera allowed control of the metered area, which was limited to a circle with a diameter equal to the length of the image scanned by the linear imaging sensor. An aperture of f 2.8 was used on the lens in front of the solid-state sensor. Both the red cloddy soil and fine sand surfaces were used. A

**TABLE 2. Illumination requirements**

| Soil | Exposure Time* (ms) | Lux | Bulb Voltage |
|---|---|---|---|
| Red cloddy | 13.3 | 1150 | 6 |
| Red cloddy | 1.2 | 36000 | 14 |
| Sand | 13.3 | 450 | 4 |
| Sand | 1.2 | 57000 | 8 |

* Maximum and minimum times recommended by the manufacturer for the CCD111.

Wagner H4651, sealed beam, quartz halogen headlight was used as the only source of illumination. The bulb was positioned 0.5 m from the soil surface at an angle of 45 degrees from vertical. Voltage on the bulb was used to control light intensity. Illumination at the maximum and minimum tolerances was measured. Table 2 summarizes the results.

Higher reflectivity in the sand surface resulted in minimum exposure with lower bulb voltage than for the red cloddy soil. The effects of variation in ambient light levels could be reduced by the supplemental bulb. The quartz halogen bulb mounted as described could be used to maintain exposure times at a minimum. Variation of bulb voltage levels, lens aperture, and exposure time may be required to obtain satisfactory performance over all conditions.

### Maximum Speed and Maximum Sampling Rates

Maximum measurable velocities are limited by the turn-around time (exposure time and digitization time) for the CCD and flash converter system. Successive images must overlap enough to permit matching. Maximum sampling rate would be limited by the exposure time plus a maximum of 500 μs required to clock one image from the CCD array. Worst-case sampling rate based on the above illumination levels would be more than once per 15 ms, or not less than 66 Hz for poorly illuminated surfaces, and once per 2 ms, or not less than 500 Hz for a well illuminated surface. Assuming the geometry of the prototype system, where the image length was 53 mm (2.0 in.) with 128-pixel overlap, maximum velocities would be 1.75 m/s (3.9 mph) for poorly illuminated surfaces and 13.2 m/s (29.4 mph) for well illuminated surfaces. Moving the imaging system further away from the surface or using wider angle lenses could significantly increase the maximum speed.

Velocity sampling rates are primarily a function of the speed at which correlations can be computed. Central processor unit (CPU) processing time will be much longer than the turn-around time for the CCD and flash converter system. The CPU processing time was measured for both the direct algorithm and the moving threshold algorithm. The direct algorithm required 207 ms with the 2 MHz 6809 processor. Velocity sampling rates would be slightly less than 5 per second. The algorithms were coded for 8 MHz versions of the Motorola 68008, 68000, and for the 16 MHz version of the Motorola 68020 microprocessors. Sampling rates would be 5, 8, and 16 per second, respectively. Times for other 8, 16, and 32-bit microprocessors would be expected to be similar. Wider bus bandwidth of the 68000 based processors did not improve performance significantly because of the large amount of 8-bit arithmetic used in the algorithms. If times nearer the maximum 66-Hz sampling rate were desired, customized hardware or digital signal processors would be required.

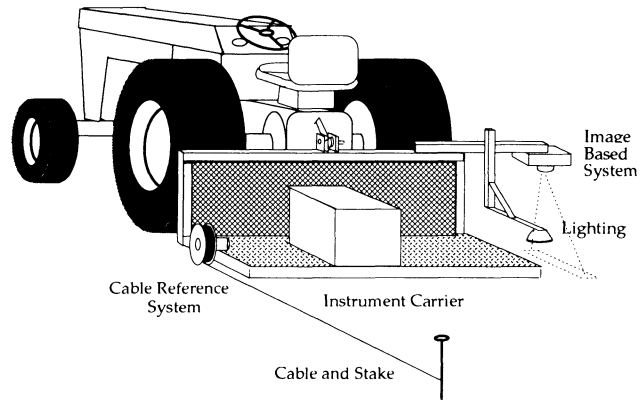


**Figure 6–Field test apparatus.**

Execution times for the moving threshold algorithm were found to be a function of displacement. Figure 5 shows results obtained with fine sand. Cloddy soil produced similar results. Execution times were reduced when displacements were small. Prior knowledge of the approximate displacement could allow significantly higher sampling rates for this algorithm. If vehicle speed were being measured, searching randomly about the best estimate of speed would minimize calculation time. Barnea and Silverman (1972) suggest using random displacements rather than a linear search.

### Field Testing

Ground tests were conducted to evaluate the performance of the system under field conditions. A schematic of the field test apparatus is shown in figure 6. The image-based system, including lighting, was attached to an instrumentation carrier which was mounted on the

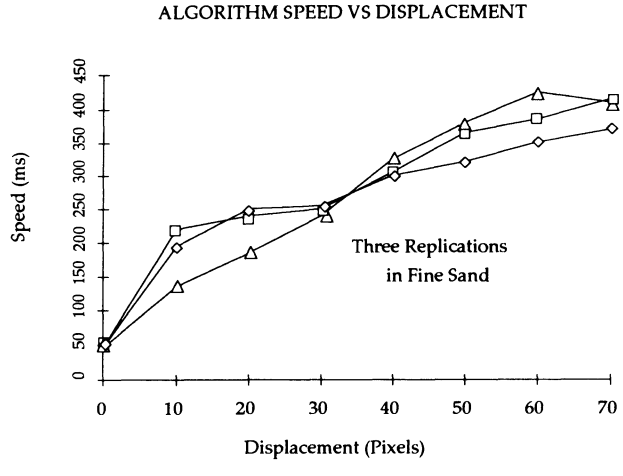


**Figure 5–Effects of displacement on algorithm speed.**

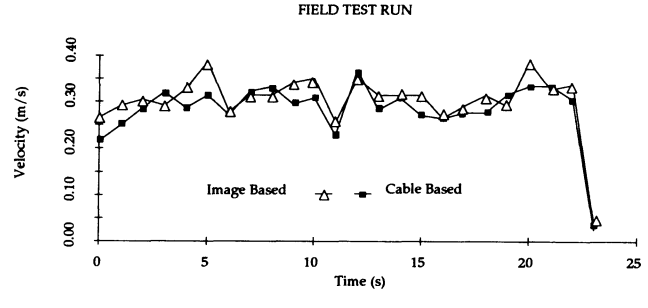


**Figure 7–Velocity profiles during a typical test run.**

**TABLE 3. Comparison of cable and image-based velocities**

| Imaging-Based Velocity vs. Cable-Based Velocity | | |
|---|---|---|
| | Image-based | Cable-based |
| Number of points | 201 | 201 |
| Average velocity | 0.47 m / s | 0.47 m / s |
| Velocity range | 0.039-1.1 m / s | 0.0031-1.0 m / s |
| Velocity S.D. | 0.64 m / s | 0.64 m / s |
| | | Difference |
| Random error (S.D.) | | 0.034 m / s |
| Most probable error | | 0.021 m / s |
| Most probable mean error | | 4.4% of average vel. |
| Estimated error in image based device | | 2.2% of average vel. |

three-point hitch of a small tractor. A velocity reference apparatus was constructed using a cable staked to the ground. The cable was unwound from a rotating drum that was fixed to the instrumentation carrier. The drum was constructed to carry one layer of a 3.2-mm (1/8-in.) steel cable. The drum was mounted on a shaft encoder, and the complete apparatus was fixed to the instrumentation carrier. A friction brake on the drum was used to maintain cable tension. At the beginning of each test run, the cable was wound onto the drum and staked.

Ten test runs were conducted with average velocities ranging from 0.2 to 1.0 m/s (0.4-2.2 mph). Data were collected as individual pairs of readings, one each from the cable-based system and the image-based system. Conventional measurements of error in velocity systems compare the measured velocity with an average velocity through a timed distance. Our study differs in that the reference velocity is measured over the same interval as the image based velocity, and the interval was kept very short (approximately 20 mm). Aperture on the imaging system was set at f 2.8 and bulb voltage level at approximately 13 V. A short bermuda grass pasture was used for the testing. Figure 7 shows results from a typical test run.

Data from all tests were combined, and a comparison of the cable and image-based velocities was made. Table 3 shows results of the comparison. The velocity range given in the table is for specific points, not averages. The lower portion of the table presents differences between cable-based measurements and image-based measurements. The most probable error for the image-based device, assuming that perfect data were obtained from the cable-based device, would be 4.4% of the average reading. An error was estimated for the image-based device by proportioning error to each of the devices based on standard deviations of their velocities. Using that estimate, error in the image-based device would be approximately 2.2% of the average velocity. The laboratory tests revealed an inaccuracy of ±2 pixels in 128 pixels, (±1.6%), or an error of ±3.2% for displacements of 64 pixels.

Figure 8 presents the actual data taken in the tests. Variations did not appear to be correlated with velocity and were distributed evenly throughout the velocity range.

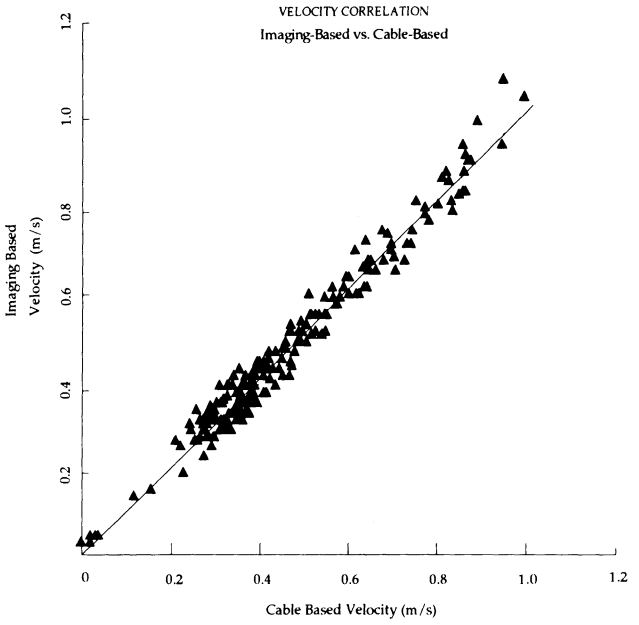


**Figure 8–Test data showing cable-based vs. image-based correlation.**

## DISCUSSION AND SUMMARY

Technical feasibility of an image-based velocity sensor was demonstrated under laboratory and limited field conditions. The sensor as developed appears to outperform undriven wheel-based measurements. The sensor has no limit on the slowest speed that can be measured and at low speeds outperforms radar systems. At higher speeds, the sensor may not be as precise as radar units. Error in velocity measurements with linear imaging velocity sensors is dependent on resolution of the sensor, provided the sensor is aligned with the direction of travel. The error in the system described here was less than 2% of the velocity reading when alignment was correct and optimum displacement between images was used. Error in field test of the unit resulted in a slightly higher error of just over 2%. Angular misalignment was limited to 0.9 degrees, allowing turning radii of 2.0 m (78 in.) for typical geometries. Side-slip misalignment was limited to 6% of the forward displacement to assure accurate readings.

Limitations of the device were found to include a constraint on the maximum velocity that can be measured, maximum number of velocity measurements that can be made per unit time, and the need for auxiliary lighting. Velocity sampling rates of 4 per second can be achieved using 8-bit microprocessors for correlation calculations. The moving threshold algorithm can be used to increase the sampling rate, but would be best used where some knowledge of velocity range is available. Maximum velocities of 13.3 m/s (29.4 mph) could be measured for the geometry used and for well illuminated surfaces. Auxiliary illumination would be required for systems based on the design. Conventional quartz halogen bulbs provide adequate illumination in dark conditions.

Many potential errors could develop in applying the image-based approach. In cases where the ground is not a stable reference, for example where moving loose soil or

blowing grass or weeds may fall within the image, a matching image may not be found or worse, a match may be found generating a false reading. In addition, the process as currently envisioned relies on a reasonably stable moving platform and does not account for significant pitch and roll changes where either no matching images may be found or errors may be induced because of pitch changes. The technique depends on gathering an unobscured image of fixed ground surfaces. Other noncontact techniques including use of doppler RADAR or ultrasonic systems suffer from the same problems. Dust obscuring the view of the camera system may be a problem. During the testing, a very dusty environment existed and the downward facing lens was little effected. Dust accumulation causing blurring of the image actually seemed to improve the performance of the system. Clearly though mud splashed over the lens could not be accommodated.

## REFERENCES


Barnea, I. J. and H. F. Silverman. 1972. A class of algorithms for fast digital image registration. *IEEE Transactions on Computers* C-21(2):179-186.

Flory, R. E. 1985. Image acquisition technology. *Proceedings of the IEEE* 73(4):613-637.

Hall C. W. 1977. *Errors in Experimentation.* Champaign, IL: Matrix Publishers, Inc.

Mussman, H. G. and H. Grallert. 1985. Advances in picture coding. *Proceedings of the IEEE* 73(4):523-548.

Sokol, D. G. 1984. Next generation radar sensor for true ground speed measurements. *Agricultural Electronics–1983 and Beyond*, 76-84. St. Joseph, MI: ASAE.

Tompkins, F. D., W. E. Hart, R. S. Freeland, J. B. Wilkerson and L R. Wilhelm. 1988. Comparison of tractor ground speed measurement techniques. *Transactions of the ASAE* 31(2):369-374.